Quantum Information and Computation, Vol. 5, No. 7 (2005) 573–582

A COMPARISON OF DECOHERENCE-FREE SUBSYSTEM/SUBSPACE FOR PARTIALLY-BROKEN SYMMETRY

SHABNAM SIDDIQUI
Department of Physics, University of Arkansas
Fayetteville, AR 72701, USA

JULIO GEA-BANACLOCHE
Department of Physics, University of Arkansas
Fayetteville, AR 72701, USA

Received February 16, 2005
Revised August 23, 2005

We study the performance of the 3-qubit decoherence-free subsystem and the 4-qubit decoherence-free subspace in the presence of partially correlated noise. We characterize their performance in terms of the average and worst-case fidelity, as a function of the ratio of the interqubit distance to the correlation length of the noise, and find that, in general, more symmetric arrangements (triangles or squares) lead to better performance. Overall, we find the 3-qubit code to perform better than the 4-qubit code by about a factor of 2 in the average infidelity. We observe that this is related to the greater robustness of this code against uncorrelated (independent) errors.

Keywords: Quantum computation, decoherence-free subspaces
Communicated by: R Cleve & A Imamoglu

1. Introduction

By now various schemes have been proposed to deal with the problem of decoherence in quantum computers [1]. Some of these schemes are: (1) Quantum error-correcting codes (QECCs) [2, 3], concatenated for fault tolerance; (2) DFS (decoherence free subsystem/subspace) [4, 5, 6]; (3) dynamical decoupling methods [7]. In the DFS scheme (see [8] for an extensive review), the information is stored in a subsystem/subspace which decouples from the environment due to symmetry between the system and the environment and therefore encoded information stays protected for a long period of time. Originally it was thought that these systems would be good candidates for quantum memory; later it was found that fault-tolerant computations [9, 10] can also be done on the DFS. Hence, these systems provide a good solution to the problem of decoherence as long as symmetry conditions can be obtained physically and maintained for a long period of time. But the symmetry conditions are stringent and difficult to obtain physically for large scale computations. In spite of this, DFSs have been considered as a good approach towards finding a solution to the problem of decoherence.

The smallest DF subsystem in which a qubit can be encoded is a three-qubit system [6, 11], whereas the smallest subspace is a four-qubit system. Therefore, the subsystem is a better candidate over the subspace in terms of lesser number of qubits requirement. In this work

we have tried to answer the following question: which of the two (subsystem/subspace) is better over the other when the symmetry conditions are partially broken. We note that the performance of decoherence-free subspaces under partially broken symmetry conditions has been considered before by other authors; see, e.g., [4] for an early example.

We have looked at the performance of three- and four-qubit DFSs in the presence of an environment that does not couple symmetrically to the qubits. This means that each qubit experiences a (slightly) different environment and therefore all the qubits experience somewhat independent errors. The degree of independence of these errors is determined by the correlation length of the noise. We show that, for finite correlation length, a three-qubit DFS code works better than a four-qubit code, by at least a factor of 2 in the "infidelity" (for small deviations from perfect symmetry) when the spatial arrangement of the qubits is optimized in both cases. This comparison assumes perfect gates are used for encoding and decoding, an assumption that is discussed further in the Conclusions section.

The layout of the paper is as follows. In Section 2 we introduce our noise model and discuss the three-qubit decoherence-free subsystem. We derive analytical expressions for both the minimum and the average infidelity, after encoding, interaction with the environment, and decoding, and we discuss the effects of different spatial arrangements of the qubits. In Section 3 the same kinds of results are presented for the four-qubit decoherence-free subspace, which is somewhat simpler because no encoding and decoding are required. Section 4 is devoted to a comparison, further discussion of the results, and conclusions.

2. 3-qubit DFS and partially-correlated noise

2.1. *Noise model*

We assume the interaction of our qubits with the environment is described by the following Hamiltonian

$$H = \sum_{i=1}^{3} \hbar g_i E_i \left(\sigma_{i+} e^{i\phi_i} + \sigma_{i-} e^{-i\phi_i} \right) \tag{1}$$

where σ_{i+} and σ_{i-} are raising and lowering operators, the g_i are coupling constants, the E_i are (real) field amplitudes, and the ϕ_i are field phases. We allow for both E_i and ϕ_i to be random, partially correlated, variables, with $\langle E_i e^{i\phi} \rangle = 0$. Perfect collective decoherence will apply if all the qubits see the same environment, that is, if all the g_i, E_i and ϕ_i are equal. We will assume all $g_i = g$, but postulate a partial correlation [13] for the random environmental fields, of the form

$$\begin{aligned} \left\langle E_i E_j e^{i(\phi_i + \phi_j)} \right\rangle &= 0 \\ \left\langle E_i E_j e^{i(\phi_i - \phi_j)} \right\rangle &= E_0^2 e^{-|\mathbf{x}_i - \mathbf{x}_j|/l} \end{aligned} \tag{2}$$

where $\mathbf{x}_i$ is the position of the i-th particle, and l is the noise correlation length. This noise becomes fully correlated when $l \gg d$ (where d is the characteristic interqubit spacing) and totally uncorrelated when $l \ll d$. Higher-order correlation functions could be introduced, by assuming, for instance, Gaussian correlations, as was done in our previous paper [13], but

for the short-time approximations used below only the second-order correlations, given by Eq. (2), will be necessary.

2.2. *Decoherence of the code*

The basis states for encoding the qubit are [6], [11], [10]:

$$|0_L\rangle = \frac{1}{\sqrt{2}}\left(|10\rangle - |01\rangle\right)|0\rangle \tag{3}$$

$$|1_L\rangle = \frac{2}{\sqrt{6}}|0\rangle\left(|10\rangle - |01\rangle\right) + \frac{1}{\sqrt{6}}\left(|10\rangle - |01\rangle\right)|0\rangle\,. \tag{4}$$

The encoded state is written as:

$$|\Psi(0)\rangle_L = \alpha\,|0\rangle_L + \beta\,|1\rangle_L \tag{5}$$

where α, β are complex coefficients and we define the real numbers a, b, γ, as:

$$\alpha = ae^{i\phi_1},\ \beta = be^{i\phi_2},\ \phi_1 - \phi_2 = \gamma \tag{6}$$

In the Schrödinger picture, the time evolution of the system is given by:

$$|\Psi(t)\rangle = U(t)\,|\Psi(0)\rangle \tag{7}$$

where

$$U(t) = e^{-iHt} = \prod_{i=1}^{3}\left(e^{-ig_iE_it(\sigma_{ix}\cos\phi_i - \sigma_{iy}\sin\phi_i)}\right) \tag{8}$$

and

$$e^{-ig_iE_it(\sigma_{ix}\cos\phi_i - \sigma_{iy}\sin\phi_i)} = \cos(g_iE_it) - i\sin(g_iE_it)\left(\sigma_{ix}\cos\phi_i - \sigma_{iy}\sin\phi_i\right) \tag{9}$$

The unitary time-evolution operator can be expanded in power series of time and for our case we considered the expansion to second order,

$$U(t) \approx 1 - it\sum_{i=1}^{3} g_iE_i\eta_i - t^2\sum_{i,j=1}^{3}\left(\frac{\delta_{ij}}{2} + \mu_{ij}\eta_i\eta_j\right)g_ig_jE_iE_j \tag{10}$$

where

$$\mu_{ij} = \begin{cases} 1 & \text{for } i \neq j, \\ 0 & \text{for } i = j. \end{cases} \tag{11}$$

and

$$\eta_i = \sigma_{ix}\cos\phi_i - \sigma_{iy}\sin\phi_i \tag{12}$$

It is characteristic of decoherence-free subsystems, as opposed to subspaces, that the overall form of the state changes, in general, under time evolution, even when the collective decoherence condition is perfectly satisfied. Accordingly, in order to determine to what extent the initially encoded information has been protected in our case, we apply a formal "decoding" procedure [11] to the time-evolved state. As explained in [11], for fully correlated noise, we expect the state of the system after time evolution and decoding to be the following:

$$|\Psi(t)\rangle = (\alpha\,|0\rangle + \beta\,|1\rangle)\,|0\rangle\,(C_0(t)\,|1\rangle + C_1(t)\,|0\rangle) \tag{13}$$

In the above equation the first and the second qubit remain unentangled with the environment whereas the third qubit gets entangled with the environment. Therefore the encoded qubit is protected against decoherence. In our case, in general, the encoded qubit and the second qubit also become entangled with the environment.

In order to evaluate the performance of the code, we trace over the third qubit of the state and that gives us:

$$\rho_{red}(t) = {}_3\langle 0|\Psi(t)\rangle\,\langle\Psi(t)|0\rangle_3 + {}_3\langle 1|\Psi(t)\rangle\,\langle\Psi(t)|1\rangle_3 \tag{14}$$

then calculate the overlap of state $|\psi_0\rangle\,|0\rangle$ with the reduced state, where $|\psi_0\rangle \equiv \alpha|0\rangle + \beta|1\rangle$. Actually this is equivalent to the sum of probabilities for finding the system in state $|\psi_0\rangle\,|00\rangle$ and $|\psi_0\rangle\,|01\rangle$. Therefore the total "success" probability (essentially, the fidelity) is given as:

$$F^2(t) = \langle\psi_0|\langle 0|\rho_{red}(t)|\psi_0\rangle|0\rangle \tag{15}$$

For three particles on a line, equally spaced by a distance d, using Eq. (1) and Eq. (2), the above expression reduces to:

$$F^2_{line}(t) = 1 - 2(gE_0t)^2\left(1 - e^{-d/l}\right)\left(1 + \frac{4}{3}a^2b^2\sin^2\gamma + \frac{4}{3}b^2e^{-d/l}\left(1 - \frac{2}{3}b^2 + \frac{2ab}{\sqrt{3}}\cos\gamma\right)\right) \tag{16}$$

Similarly, for the three particles on an equilateral triangle of length d we obtain the following:

$$F^2_{tri}(t) = 1 - 2(gE_0t)^2\left(1 - e^{-d/l}\right)\left(1 + \frac{4}{3}a^2b^2\sin^2\gamma\right) \tag{17}$$

It is easily seen that both expressions reduce to unity for perfectly correlated noise ($l \to \infty$). For intermediate cases, the fidelity naturally depends on the initial state. Two natural measures of the code performance are then the average fidelity and the "worst-case" fidelity.

2.2.1. *Average fidelity*

The expression for the average fidelity is obtained by taking the integral of $P(t)$ over the surface area of the Bloch sphere, that is, over all values of α and β with the constraint $|\alpha|^2 + |\beta|^2 = 1$. The natural measure is then $(1/4\pi)\sin\theta\,d\theta\,d\gamma$, with $a = \cos\theta/2$ and $b = e^{i\gamma}\sin\theta/2$, and $0 \le \theta \le \pi$, $0 \le \gamma \le 2\pi$. The result is

$$F^2_{line}(t) = 1 - \frac{20}{9}(gE_0t)^2\left(1 - \frac{e^{-2d/l}}{3} - 2\frac{e^{-d/l}}{3}\right) \tag{18}$$

$$F_{tri}^2(t) = 1 - \frac{20}{9}(gE_0t)^2(1 - e^{-d/l}) \tag{19}$$

The corresponding "infidelities," scaled by $(gE_0t)^2$, are shown in Figure 1, as functions of d/l. For the case where deviations from perfect collective decoherence are small ($d \ll l$), insight can be gained from the power series expansions of Eq. (18) and Eq. (19), which go as

$$F_{line}^2(t) \simeq 1 - \frac{20}{9}(gE_0t)^2\frac{4d}{3l} = 1 - 2.96(gE_0t)^2\frac{d}{l} \tag{20}$$

and

$$F_{tri}^2(t) \simeq 1 - \frac{20}{9}(gE_0t)^2\frac{d}{l} = 1 - 2.22(gE_0t)^2\frac{d}{l} \tag{21}$$

respectively.

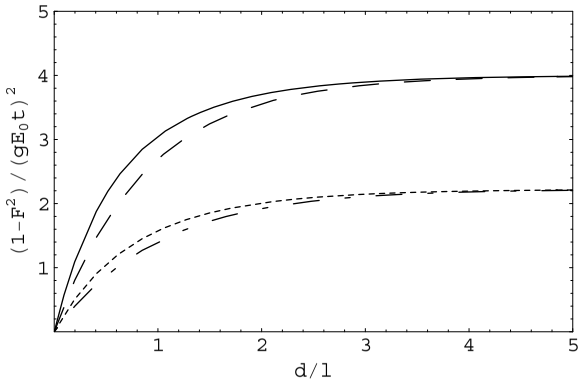

Fig. 1. Average infidelity, divided by $(gE_0t)^2$, vs. interqubit distance (in units of the noise's correlation length) for the 3-qubit DFS, with the qubits arranged in a triangle (dash-dotted line) and on a line (dotted line), and for the 4-qubit DFS with the qubits arranged in a square (dashed line) and on a line (solid line).

2.2.2. *Worst-case fidelity*

Alternatively, one can calculate the fidelity for the values of α and β for which the expressions in Eq. (16) and Eq. (17) are minimum. For the case of three particles on a line, this is :

$$\begin{aligned} F_{line}^2(t) &= 1 - 8(gE_0t)^2\left(\frac{-1 + e^{d/l}}{-1 + 3e^{d/l}}\right) \\ &\simeq 1 - (gE_0t)^2\frac{4d}{l} \end{aligned} \tag{22}$$

where the second line shows, as before, the result of expanding in powers of d/l. This expression was obtained for the following parameters:

$$b = \frac{\sqrt{3/2\left(e^{d/l} + e^{2d/l}\right)}}{3 - 2e^{-d/l} + e^{-2d/l}},\ \gamma = \cos^{-1}\left(\frac{be^{-d}}{a\sqrt{3}}\right) \tag{23}$$

Similarly, for the triangle we obtain the following expression:

$$F_{tri}^2(t) = 1 - \frac{8}{3}(gE_0t)^2\left(1 - e^{-d/l}\right)$$
$$\simeq 1 - (gE_0t)^2\frac{8d}{3l} = 1 - 2.67(gE_0t)^2\frac{d}{l} \tag{24}$$

where

$$b = \pm\sqrt{\frac{1}{2}},\ \gamma = \pi/2 \tag{25}$$

By looking at the expressions for average and worst cases of a three qubit on a line and triangle, one can say that the symmetry in the arrangement of qubits reduces decoherence to some extent. The results for F_{line}^{min} and F_{tri}^{min} are plotted in Fig. 2 as functions of d/l. For small d/l, they are actually not very different from the average fidelity results (18) and (19), as the power series expansions show.

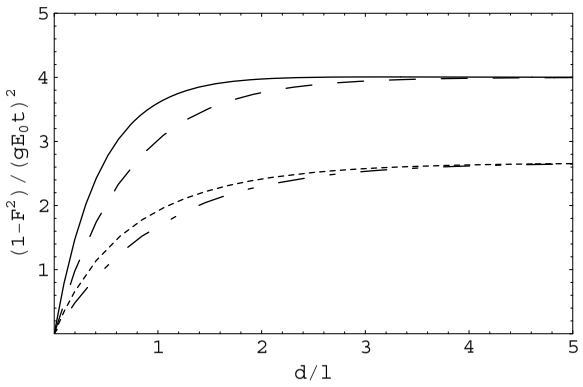

Fig. 2. Worst-case infidelity, divided by $(gE_0t)^2$, vs. interqubit distance (in units of the noise's correlation length) for the 3-qubit DFS, with the qubits arranged in a triangle (dash-dotted line) and on a line (dotted line), and for the 4-qubit DFS with the qubits arranged in a square (dashed line) and on a line (solid line).

3. 4-qubit DFS

3.1. *Basis states and fidelity*

The four-qubit code [4], [5] belongs to the smallest decoherence-free subspace. This code provides full protection against correlated noise and it has been shown in [9] that one can do fault-tolerant computations in this subspace as long as symmetry conditions are maintained. We have looked at the performance of this code in the presence of partially correlated noise, using the same noise model as in Section 2.

The basis states for the code are:

$$|0_L\rangle = \frac{1}{2}\left(|0110\rangle + |1001\rangle - |0011\rangle - |1100\rangle\right) \tag{26}$$

$$|1_L\rangle = \frac{1}{\sqrt{3}}\left(|1010\rangle + |0101\rangle - \frac{1}{2}\left(|0011\rangle + |1100\rangle + |0110\rangle + |1001\rangle\right)\right) \tag{27}$$

These states can also be written in the following form:

$$|0_L\rangle = |J=0,\lambda=0,m_j=0\rangle = \frac{1}{2}\left(|0\rangle_1|1\rangle_3 - |1\rangle_1|0\rangle_3\right)\left(|1\rangle_2|0\rangle_4 - |0\rangle_2|1\rangle_4\right) \tag{28}$$

$$\begin{aligned}|1_L\rangle = |J=0,\lambda=1,m_j=0\rangle = &\frac{1}{\sqrt{12}}\Big(\left(|1\rangle_1|0\rangle_2 - |0\rangle_1|1\rangle_2\right)\left(|1\rangle_3|0\rangle_4 - |0\rangle_3|1\rangle_4\right)\\ &+ \left(|0\rangle_2|1\rangle_3 - |1\rangle_2|0\rangle_3\right)\left(|1\rangle_1|0\rangle_4 - |0\rangle_1|1\rangle_4\right)\Big)\end{aligned} \tag{29}$$

These basis states are eigenstates of total angular momentum $J=0$ for four spin-$\frac{1}{2}$ systems. The states are described by three quantum numbers J,λ,m_j, where J and m_j are the total angular momentum and magnetic number, and λ describes the way the spins are added to give total $J=0$. $\lambda=0$ is obtained by adding the spins in pairs to give zero angular momentum, and $\lambda=1$ is obtained by adding them in pairs to give 1 unit of angular momentum, and then adding the pairs to get zero J.

For four particles on a line, each separated from the next one by a distance d, the expression for the fidelity of the code is:

$$F^2_{line}(t) = 1 - 4(gE_0t)^2\left(1-e^{-d/l}\right)\left(\left(1+e^{-d/l}\right)\left(1+e^{-d/l}\frac{ab}{3}\cos\gamma\right) - b^2\left(e^{-d/l} - \frac{e^{-2d/l}}{3}\right)\right) \tag{30}$$

The expression for four qubits arranged in a square of length d is:

$$F^2_{sq.}(t) = 1 - 4(gE_0t)^2\left(1 - e^{-d/l} + \left(e^{-d/l} - e^{-\sqrt{2}d/l}\right)\left(\frac{2}{3}b^2 + \frac{ab}{\sqrt{3}}\cos\gamma\right)\right) \tag{31}$$

3.1.1. *Average fidelity*

As we did in Section 2, we can average Eq. (30) and (31) over the whole Bloch sphere to get the average fidelity:

$$\begin{aligned}F^2_{line}(t) &= 1 - 4(gE_0t)^2\left(1 - \frac{1}{6}\left(3e^{-d/l} + 2e^{-2d/l} + e^{-3d/l}\right)\right)\\ &\simeq 1 - 4(gE_0t)^2\frac{5d}{3l} = 1 - 6.67(gE_0t)^2\frac{d}{l}\end{aligned} \tag{32}$$

$$\begin{aligned}F^2_{sq.}(t) &= 1 - 4(gE_0t)^2\left(1 - \frac{1}{3}\left(2e^{-d/l} + e^{-\sqrt{2}d/l}\right)\right)\\ &\simeq 1 - 4(gE_0t)^2\frac{(2+\sqrt{2})d}{3l} = 1 - 4.55(gE_0t)^2\frac{d}{l}\end{aligned} \tag{33}$$

These functions are plotted in Figure 1 (solid and dashed lines, respectively).

3.1.2. *Worst Case Fidelity*

The worst-case fidelity for the four qubits on a line, Eq. (30), is given by

$$\begin{aligned} F^2_{line}(t) &= 1 - \frac{4}{6}(gE_0t)^2(1-e^{-d/l})\Big(6 + e^{-2d/l}(1+3e^{d/l}) \\ &+ \frac{(1-e^{-d/l})}{\sqrt{1+3e^{2d/l}}}\left((1+e^{-d/l})^2 - 4\right)\Big) \\ &\simeq 1 - 4(gE_0t)^2\frac{21d}{12l} = 1 - 6.75(gE_0t)^2\frac{d}{l} \end{aligned} \tag{34}$$

and it is obtained for

$$b = \frac{1}{2}\sqrt{2 - \frac{1-3e^{d/l}}{\sqrt{1+3e^{2d/l}}}} \tag{35}$$

For the square the result is:

$$\begin{aligned} F^2_{sq.}(t) &= 1 - 4(gE_0t)^2\left(1 - e^{-\sqrt{2}d/l}\right) \\ &\simeq 1 - 4(gE_0t)^2\frac{\sqrt{2}d}{l} = 1 - 5.66(gE_0t)^2\frac{d}{l} \end{aligned} \tag{36}$$

and it is obtained for

$$b = \frac{\sqrt{3}}{2} \tag{37}$$

These results are plotted in Fig. 2, as the solid and dashed lines, respectively.

4. Results and Conclusions

Comparing the results of Sections 2 and 3, we observe the following:
(1) For small d/l (the region where the codes are likely to be useful), the average infidelity for the 3-qubit code is smaller by a factor of at least 2 than for the 4-qubit code (compare Eq. (20) to (32), or (21) to (33)). For the worst-case infidelity, one also finds a factor of ~ 2 advantage of the three-qubit code when the optimal arrangements (triangle and square, respectively) are compared (Eqs. (24) and (36)). This makes it a better code over the 4-qubit code, in terms of lesser number of qubits requirement as well as lesser infidelity.
(2) The better performance of the 3-qubit code is not simply a consequence of having fewer qubits (so that, when the errors are partIy independent, there are, overall, fewer chances for them to occur): rather, the performance *per qubit* (as measured, e.g., by the infidelity per qubit) appears to be better. One can see this most clearly by comparing the expressions for both codes in the limit of totally independent errors ($d/l \to \infty$). In this case, the infidelity for the 4-qubit code is $4(gE_0t)^2$, regardless of the initial state, whereas for the 3-qubit code the infidelity depends on the value of α and β, and for real α and β it is only equal to $2(gE_0t)^2$. This means that (at least, for some special initial states) the 3-qubit DFS is less sensitive than the 4-qubit DFS to certain kinds of single-qubit errors. Note that, in the independent-error limit, the operator (10) may be thought of as causing any of the errors $\{\sigma_{ix}, \sigma_{iy}\}$ randomly,

with probability $\frac{1}{2}(gE_0t)^2$. Any of these errors, acting on the 4-qubit code, produces a totally orthogonal state, and hence a zero fidelity; yet, when they act on the 3-qubit code, the resultant states have typically a nonvanishing projection on the initial state.

Finally, let us note that, in practice, a possibly very important factor that the above comparison does not take into account is the number of operations needed to work with the two codes. In particular, the procedure for encoding and decoding the information in the 3-qubit code described in [11], which we have followed here, is rather laborious, and one might naturally be concerned about the errors introduced through the imperfect operation of all the gates involved. It is beyond the scope of the paper to address this question in detail, since to do it properly one would have to compare, not only the encoding and decoding (which, in principle, only need to be done at the beginning and the end of the computation), but, more importantly, the relative difficulty of performing fault-tolerant gates (including possibly those required for error correction) on the two codes. This will naturally depend, among other things, on the particular form of the interaction that is physically available. See [14] for an example of this kind of analysis, for the two codes considered here, and for the specific case of the exchange interaction.

Acknowledgements

This research has been supported by the Army Research Office.

References

1. M. A. Nielsen and I. L. Chuang (2000), *Quantum Computation and Quantum Information*, Cambridge University Press.
2. P. Shor (1995) *Scheme for reducing decoherence in quantum computer memory*, Phys. Rev. A **52**, pp. R2493–R2496.
3. C. H. Bennett, D. P. DiVincenzo, J. A. Smolin, and W. K. Wootters (1996) *Mixed-state entanglement and quantum error correction*, Phys. Rev. A **54**, pp. 3824–3851.
4. P. Zanardi and M. Rasetti (1997) *Noiseless Quantum Codes*, Phys. Rev. Lett. **79**, pp. 3306–3309.
5. D. A. Lidar, I. L. Chuang and K. B. Whaley (1998) *Decoherence-Free Subspaces for Quantum Computation*, Phys Rev.Lett. **81**, pp. 2594–2597.
6. E. Knill, R. Laflamme, and L. Viola (2000) *Theory of Quantum Error Correction for General Noise*, Phys. Rev. Lett. **84**, pp. 25252528.
7. L. Viola and S. Lloyd (1998) *Dynamical suppression of decoherence in two-state quantum systems*, Phys. Rev. A, **58**, pp. 2733–2744.
8. D. A. Lidar and K. B. Whaley (2003) *Decoherence-Free Subspaces and Subsystems*, arXiv:quant-phys/0301032 (published as a book chapter in *Irreversible Quantum Dynamics*, F. Benatti and R. Floreanini (Eds.), pp. 83–120 (Springer Lecture Notes in Physics vol. 622, Berlin, 2003)).
9. J. Kempe, D. Bacon, D. A. Lidar and K. B. Whaley (2001) *Theory of decoherence-free fault-tolerant universal quantum computation*, Phys. Rev. A **63**, 042307.
10. D. P. DiVincenzo, D. Bacon, J. Kempe, G. Burkard and K. B. Whaley (2000) *Universal quantum computation with the exchange interaction*, Nature, **408**, pp. 339–342.
11. C.-P. Yang and J. Gea-Banacloche (2001) *Three-qubit quantum error-correction scheme for collective decoherence*, Phys. Rev. A **63**, 022311.
12. P. Zanardi (1998) *Dissipation and decoherence in a quantum register*, Phys. Rev. A **57**, 3276–3284.
13. J. P. Clemens, S. Siddiqui, J. Gea-Banacloche (2004) *Quantum error correction against corre-*

lated noise, Phys. Rev. A **69**, 062313.

14. M. Hsieh, J. Kempe, S. Myrgren and K. B. Whaley (2003) *An Explicit Universal Gate-set for Exchange-Only Quantum Computation*, Quantum Information Processing, **2**, 289–307 (quant-ph/0309002).